Biomacromolecules

WILLIAM & MARY

Subscriber access provided by Swem Library | College of William and Mary & VIVA (Virtual Library of Virginia)

Article

Macromolecular Sensing of RNAs by Exploiting Conformational Changes in Supramolecular Nanostructures

So-hee Han, Hee-won Kim, Woo-jin Jeong, and Yong-beom Lim

Biomacromolecules, **Just Accepted Manuscript** • DOI: 10.1021/bm500480y • Publication Date (Web): 22 May 2014

Downloaded from http://pubs.acs.org on May 27, 2014

Just Accepted

"Just Accepted" manuscripts have been peer-reviewed and accepted for publication. They are posted online prior to technical editing, formatting for publication and author proofing. The American Chemical Society provides "Just Accepted" as a free service to the research community to expedite the dissemination of scientific material as soon as possible after acceptance. "Just Accepted" manuscripts appear in full in PDF format accompanied by an HTML abstract. "Just Accepted" manuscripts have been fully peer reviewed, but should not be considered the official version of record. They are accessible to all readers and citable by the Digital Object Identifier (DOI®). "Just Accepted" is an optional service offered to authors. Therefore, the "Just Accepted" Web site may not include all articles that will be published in the journal. After a manuscript is technically edited and formatted, it will be removed from the "Just Accepted" Web site and published as an ASAP article. Note that technical editing may introduce minor changes to the manuscript text and/or graphics which could affect content, and all legal disclaimers and ethical guidelines that apply to the journal pertain. ACS cannot be held responsible for errors or consequences arising from the use of information contained in these "Just Accepted" manuscripts.

ACS Publications
High quality. High impact.

Biomacromolecules is published by the American Chemical Society. 1155 Sixteenth Street N.W., Washington, DC 20036

Published by American Chemical Society. Copyright © American Chemical Society. However, no copyright claim is made to original U.S. Government works, or works produced by employees of any Commonwealth realm Crown government in the course of their duties.

Macromolecular Sensing of RNAs by Exploiting Conformational Changes in Supramolecular Nanostructures

*So-hee Han, Hee-won Kim, Woo-jin Jeong, and Yong-beom Lim**

Translational Research Center for Protein Function Control and Department of Materials Science & Engineering, Yonsei University, Seoul 120-749, Korea

ABSTRACT

Here, we report on a ratiometric fluorescence biosensor based on self-assembled peptide nanostructures (SPN), which can respond to conformational changes induced by RNA ligand binding. The design of the SPN biosensor was inspired by the conformational stabilization and multimerization behaviors of the HIV-1 Rev protein induced by cooperative protein-protein and protein-RNA interactions. Because conformation-sensitive SPN biosensors can orchestrate binding and signal transduction events, they can be developed as highly sophisticated and smart nanomaterials for biosensing.

KEYWORDS: self-assembly, conformational change, biosensors, peptides, cooperative interaction

INTRODUCTION

The detection of biological analytes by fluorescent biosensors has been a topic of considerable research interest.[1-11] Biosensors consist of two primary functional units; a receptor that binds to a ligand and a transducer that converts the binding event into a measurable signal. Coordinated coupling of the binding and signal transduction events should provide an efficient mechanism for sensing and signal amplification.

Such a signal relay system can be found in proteins. Typically, the folded state of proteins is marginally more stable than the unfolded state, with a $\Delta G_{folding}$ of only approximately -5 to -10 kcal/mol.[12] Therefore, many proteins show highly dynamic properties and undergo conformational changes upon ligand binding.[13-15] The resulting downstream consequence of the ligand binding is the transmission of a signal to another biomacromolecules as a part of a series of signal transduction cascades.

Peptides, as the building blocks of proteins, can be made to self-assemble into supramolecular nanostructures following the proper control of molecular properties and the environment.[16-24] The size and complexity of self-assembled peptide nanostructures (SPN) might then be comparable with those of natural proteins or protein complexes.[25] Here, we report on the construction of an SPN-based protein-like dynamic biosensor, which can respond to conformational changes induced by RNA ligand binding. This SPN macromolecular sensing system combines the concept of dynamic self-assembly, conformational change of helix-coil transition, and allostery.

EXPERIMENTAL SECTION

Materials. Fmoc-amino acids and coupling reagents were purchased from Novabiochem (Germany) and Anaspec (U.S.A.). General chemicals were obtained from Sigma-Aldrich (U.S.A.) and Merck (Germany). Stearic acid was purchased from Sigma-Aldrich. High-performance liquid chromatography (HPLC) solvents were purchased from Fisher Scientific (U.S.A.). Oligonucleotides were purchased from Integrated DNA Technologies. Yeast tRNA (Am7119) was purchased from Ambion.

Peptide Synthesis. Standard amino acid protecting groups were employed for the peptide synthesis. The peptide was synthesized on Rink Amide MBHA resin LL (Novabiochem). Amino acids couplings were performed on a Tribute peptide synthesizer on a 0.1 mmol scale (Protein Technologies). For the labeling of pyrene fluorophore, the N-terminal Fmoc group of the resin-bound peptide was deprotected with 20% piperidine. Then, pyrene butyric acid (Sigma Aldrich) was coupled to the N-terminal α-amine using *O*-(benzotriazol-1-yl)-*N,N,N′,N′*-tetramethyluronium hexafluorophosphate (HBTU) and *N,N*-diisopropylethylamine (DIPEA). For final deprotection and cleavage from the resin, the resin-bound peptide was treated with a cleavage cocktail [trifluoroacetic acid (TFA)/triisopropylsilane (TIS)/water] (95:2.5:2.5) for 3 h, followed by trituration with *tert*-butyl methyl ether. The peptides were purified by reverse phase HPLC (water−acetonitrile with 0.1% TFA). The molecular weight was confirmed by matrix-assisted laser desorption/ionization time-of-flight (MALDI-TOF) mass spectrometry (Microflex LRF20, Bruker). α-Cyano-4-hydroxycinnamic acid (CHCA) was used as a matrix. The concentration was determined spectrophotometrically in water/acetonitrile (1:1) using the molar

extinction coefficient of pyrene (38459 M^{-1} cm^{-1}) at 341 nm. The extinction coefficient was based on the manufacturer's (Sigma Aldrich) information.

CD Spectroscopy. Circular dichroism (CD) spectra were measured using a Chirascan CD spectrometer equipped with Peltier temperature controller (Applied Photophysics). The peptide concentration was typically 1 μM unless otherwise noted. Sample solutions were incubated for at least 1 day before measurement. Spectra were recorded from 260 to 190 nm using the 2 mm path-length cuvettes at 25 °C. Typically, scans were repeated ten times and averaged. Molar ellipticity was calculated per amino acid residue.

Fluorescence Spectroscopy. Fluorescence spectra were measured using an LS55 Fluorescence spectrometer (PerkinElmer). Pyrene was excited at 341 nm, and the emission spectrum was collected from 360 to 550 nm. To ensure that the peptide assemblies were in thermodynamic equilibrium, peptides were sonicated for 15 min, and incubated overnight. For the RNA sensing experiment, the polynucleotide solutions were prepared in separate microcentrifuge tubes. The Rev-SBS peptide concentration was 1 μM. The molar concentration of the tRNA and ssDNA was converted relative to that of IIB RNA to maintain a similar charge ratio of peptide to polynucleotides, i.e., [tRNA] = 143000/25000 (molecular weight ratio) × [IIB RNA] and [ssDNA] = 44/25 (ratio for the number of bases) × [IIB RNA]. The peptide solution was slowly added to the polynucleotide solution to ensure homogeneous mixing. Mixed samples (Rev-SBS SPN/polynucleotides complexes) were incubated overnight and fluorescence measurements were performed at room temperature. The peptide to IIB RNA molar ratio was 20:1 unless otherwise noted.

Atomic Force Microscopy. For atomic force microscopy (AFM), approximately 2 μL of the sample was deposited onto a freshly cleaved mica surface. After the sample dried completely, residual salt was removed with distilled water while blowing with a stream of argon gas. The images were obtained in tapping mode with a Nanoscope IV instrument (Digital Instruments). AFM scans were taken at a set point of 1.2−1.5 V and a scanning speed of 0.5-1 Hz.

Wide-Angle X-ray Scattering (WAXS). X-ray scattering experiments were performed with the 4C SAXS II beamline (BL) of Pohang Accelerator Light Source (PAL), Korea. A light source from an in-vacuum Undulator 20 (IVU 20: 1.4 m length, 20 mm period) of the Pohang Light Source II storage ring was focused with a vertical focusing toroidal mirror coated with rhodium and monochromatized with a Si (111) double crystal monochromator (DCM), yielding an X-ray beam wavelength of 0.675 Å. The samples were mounted in solution sample cells with a mica window 10 μm in thickness, a volume of 50 μL, and X-ray beam path length of 0.8 mm, followed by irradiation with an exposure time of 30 s at room temperature. Scattered radiations were acquired using a two-dimensional (2D) charge-coupled detector (Mar USA, Inc.) positioned 0.2 m ($0.21\ Å^{-1} < q < 2.83\ Å^{-1}$) away from the sample.

RESULTS AND DISCUSSION

Our design of a conformation-sensitive SPN biosensor was inspired by the human immunodeficiency virus type-1 (HIV-1) Rev protein.[26] Rev is responsible for the nucleocytoplasmic export of viral RNA after binding to Rev response element (RRE) RNA. Initially, the arginine-rich motif (ARM) of Rev binds to the high-affinity site known as stem-loop IIB (~30 nt) within the large RRE (~350 nt) structure that consists of multiple stem-loops.[27,28] The IIB binding event induces a conformational change in Rev by the induced-fit mechanism, which is followed by the stabilization of an α-helical hairpin structure (Figure 1b).[29-32] The stabilization of this structure initiates the formation of hydrophobic dimerization interfaces (the head and tail surfaces; Figure S2) and subsequent V-shaped dimers. Then, more Rev proteins with V-shaped dimers as structural units can bind to low affinity sites in other stem-loops via cooperative protein-protein and protein-RNA interactions.[33,34] As many as 10-12 Rev proteins can multimerize along a single RRE.[26,34]

Monomeric Rev-based peptides have been the subject of considerable research in large part because of the development of inhibitors that target HIV-1 protein-RNA interactions. Regarding Rev peptides that have the propensity to aggregate, we previously showed that the Rev-based peptide spanning the ARM and oligomerization domains of the Rev protein could self-assemble and form α-helix-stabilized nanostructures when chemically functionalized with a hydrophobic alkyl chain.[35] The self-assembly process is highly dependent on the environmental conditions such as ionic strength.

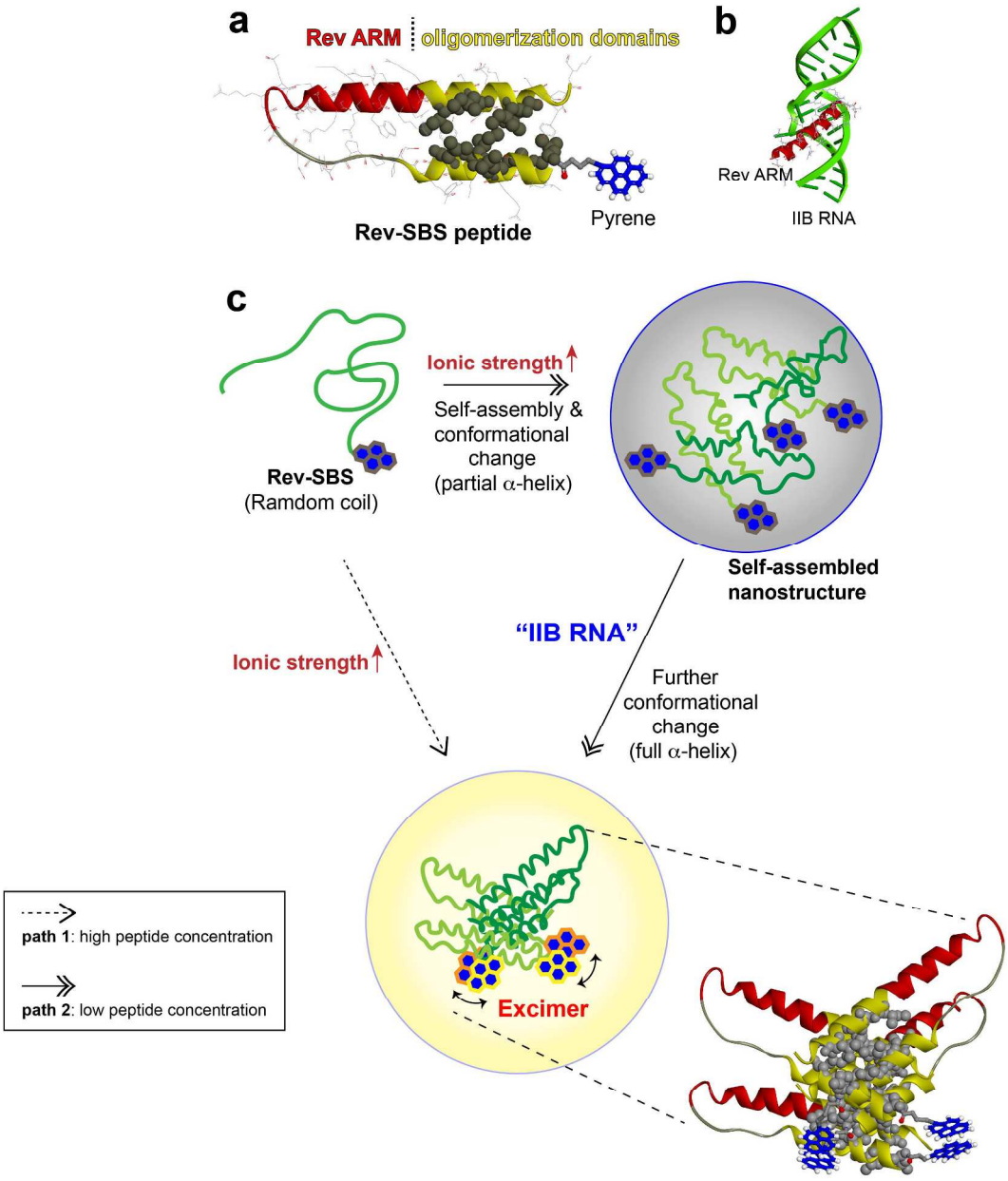

Figure 1. a) Rev-SBS self-assembling peptide building block. b) Structure of the Rev ARM peptide and RRE IIB RNA (PDB ID = 1ETF).[32] c) Mechanism of RNA sensing by the conformation-sensitive self-assembled peptide nanostructure biosensor. Hydrophobic residues important for self-assembly are shown in grey.

Based on the aforementioned properties of the Rev protein and Rev-based peptides, the peptide building block for the self-assembly into a conformation-sensitive RNA biosensor was designed. The designed Rev-SBS (Rev Self-assembled BioSensor) peptide consisted of an ARM domain flanked by two oligomerization domains (Figure 1a; Figures S1 and S2). Pyrene was conjugated at the N-terminus to provide a mechanism for self-assembly by hydrophobic and π–π stacking interactions and for fluorescence detection.

We first investigated the dependence of Rev-SBS's conformation on the change in ionic strength. As shown in Figure 2a, the peptide was stabilized in an α-helical structure when the ionic strength of the solution was increased to 150 mM, as shown by the significant increase in the molecular ellipticity at 208 and 222 nm. Quantitatively, the $[\theta]_{222}/[\theta]_{208}$ ratios shifted from 0.31 in water to 0.70 in 150 mM salt. This ratio is a measure of helicity, and increasing values correspond to the increasing degree of the α-helix.[36] The degree of helix stabilization increased in a gradual fashion as the ionic strength increased (Figure S9). The result can be explained by the stabilization of the Rev α-helical hairpin structure, which was induced by molecular self-assembly.[35] The increased ionic strength can fortify hydrophobic interactions at the intra- and intermolecular interfaces of the peptide for V-shaped hairpin dimer formation followed by multimerization via cooperative protein-protein interactions.[30,33,35,37,38] Conformation of Rev-SBS peptide was also affected by changes in temperature and pH, indicating that the peptide has highly dynamic structure (Figure S11 and S12).

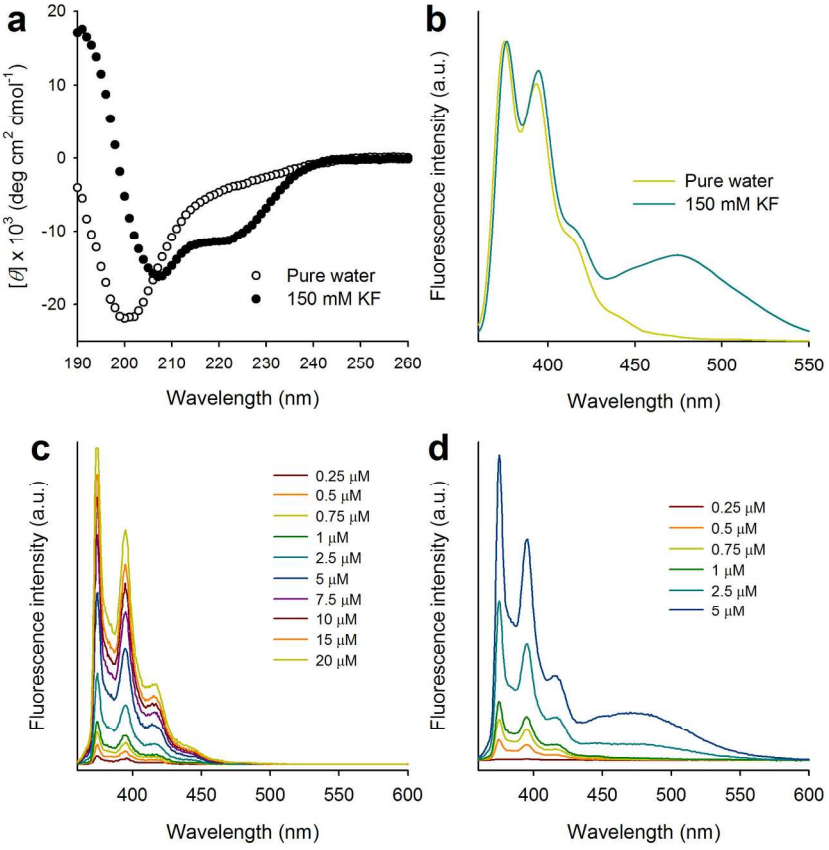

Figure 2. a) Circular dichroism (CD) and b) fluorescence emission spectra of Rev-SBS. [Rev-SBS] = 15 μM. Concentration-dependent fluorescence spectra of Rev-SBS c) in pure water and d) in 150 mM KF. All the measurements were performed at *r.t.*

Interestingly, we observed the formation of a pyrene excimer in the high ionic strength condition (Figure 2b). The excimer is an excited dimer of pyrene that forms when two pyrene molecules are spatially proximal, with the signal strength dependent on the distance.[1,39] Therefore, this result indicated that pyrene fluorophores became proximal due to the self-assembly-induced dimer/multimer formation (Figure 1c). When the peptide was dissolved in pure water, excimer formation could not be observed even at the higher concentrations of peptide

tested (Figure 2c and Figure S14). At a fixed ionic strength of 150 mM, the excimer formation was dependent on the concentration of the Rev-SBS peptide (Figure 2d and Figure S14).

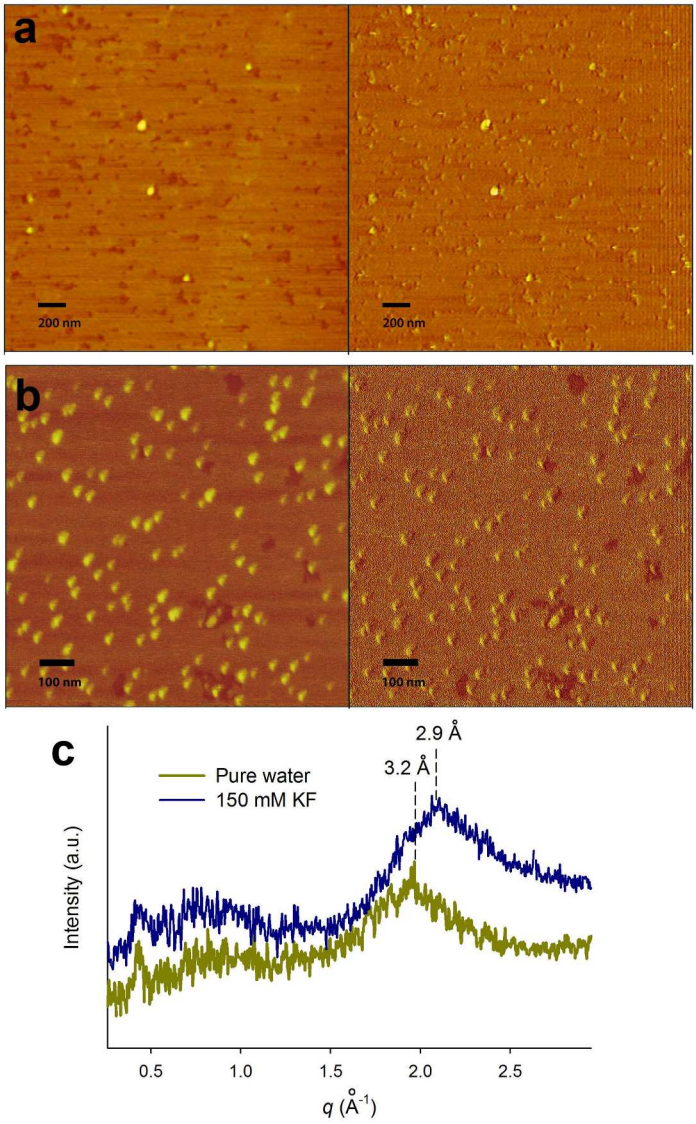

Figure 3. a) AFM image of Rev-SBS in pure water. [Rev-SBS] = 2.5 μM. b) AFM image of Rev-SBS in 150 mM KF. [Rev-SBS] = 1 μM. Left: height image, Right: phase image. c) WAXS data. [Rev-SBS] = 50 μM.

Next, we examined the aggregation status and morphology of the Rev-SBS peptide. In pure water, the Rev-SBS peptide was found to exist mostly in a monomolecular state, and to coexist

with a small population of aggregated nano-objects (Figure 3a). In stark contrast, discrete and globular nano-objects (d = ~20-50 nm) were the sole species when the peptide was dissolved under high ionic strength conditions (Figure 3b). These data further show that the efficient self-assembly of the Rev-SBS peptide occurs only at high ionic strength. Wide-angle X-ray scattering (WAXS) data of Rev-SBS in solution showed that the reflection corresponding to a d-spacing of 3.2 Å (in pure water) shifted to 2.9 Å with a concomitant increase in signal intensity (in 150 mM KF). These data indicate that there is a certain structural transition of the Rev-SBS SPN that induces self-assembly and helix stabilization when the ionic strength is increased.

Taken together, the results suggest the physical coupling of self-assembly, helix stabilization, and pyrene excimer formation, all of which have a positive correlation with ionic strength and peptide concentration. We then wanted to determine the possibility of developing a conformation-sensitive RNA biosensor utilizing the physical coupling behavior in the SPN of the Rev-SBS peptide. To maximize the dynamic range, the concentration of the peptide was fixed at a low concentration of 1 μM, at which the peptide was shown to efficiently aggregate into nano-objects but have a relatively weak excimer signal (Figure 4b & Figure S7).

Figure 4a shows the conformational status of the Rev-SBS peptide before and after binding to IIB RNA. Before binding to IIB, the degree of helix stabilization was moderate ($[\theta]_{222}/[\theta]_{208}$ ratio = 0.65). However, a difference spectrum for the Rev-SBS peptide revealed that the significant stabilization of the α-helix occurred after IIB binding ($[\theta]_{222}/[\theta]_{208}$ ratio = 1.15). For the difference spectrum, we subtracted the IIB RNA spectrum from the peptide-IIB RNA complex spectrum. Thus, the result indicated an induced-fit helical conformational change of the Rev-SBS peptide after IIB RNA binding. The spherical morphology of SPN was maintained, but the overall size was increased after the RNA binding (Figure S8). The concomitant change that

accompanied the RNA-induced helix stabilization was an increase in the emission intensity of the pyrene excimer (Figure 4b). This change is consistent with the results observed when the ionic strength was increased (*vide ante*).[35] Therefore, the IIB RNA binding event induces a conformational change in the Rev-SBS nanostructures that make pyrene fluorophores spatially proximal. The ratio of pyrene excimer emission (I_e, 480 nm) to pyrene monomer emission (I_m, 373 nm) was used as a quantitative measure of the signal.[40] The fold difference in the I_e/I_m ratio between the signals in the presence and the absence of IIB RNA (i.e., dynamic range) was up to ~4.5 under the experimental conditions tested (Figure 4b).

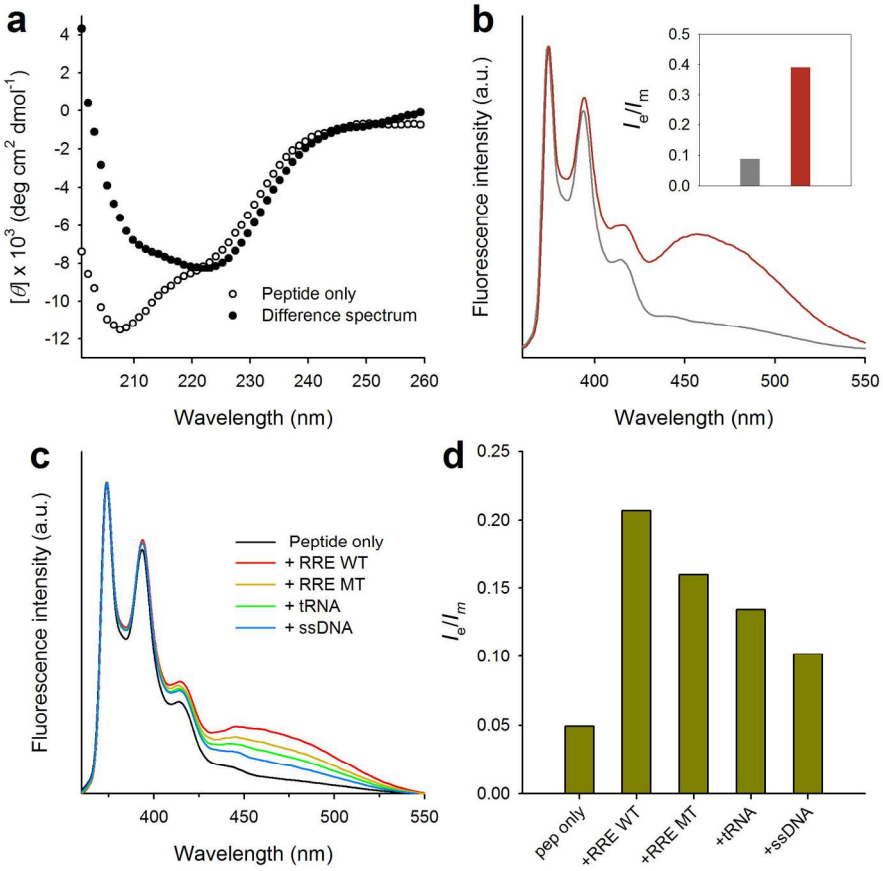

Figure 4. Conformation-sensitive SPN biosensor. (a) Conformation of the Rev-SBS peptide before (◦) and after (●) IIB RNA binding. (b) Normalized fluorescence emission spectra of Rev-

SBS before (black) and after (red) binding to IIB RNA. [Rev-SBS] = 1 μM, [IIB RNA] = 0.5 μM in Hepes Buffered Saline (KCl, 150 mM). (c) Normalized fluorescence emission spectra of Rev-SBS after the addition of different types of polynucleotides. [Rev-SBS] = 1 μM. (d) Quantification of the fluorescence signal.

Having established the possibility of detecting IIB RNA binding using the Rev-based SPN, we then investigated the selectivity of the Rev-SBS SPN biosensor. The data show that the biosensor can effectively discriminate tRNA from IIB RNA (Figure 4c, d). The selectivity for single stranded DNA (ssDNA; T7 DNA) was even greater than that for the tRNA. The biosensor could also distinguish a wild-type IIB RNA from a single base-pair mutant of IIB RNA (G46-C74 to C46-G74; Figure S3); the mutation selected has been shown to be important for Rev binding.[41] The selectivity of the biosensor was greatest in 150 mM salt, indicating the importance of ionic strength for both optimal biosensor performance and self-assembly (Figure S10).

CONCLUSIONS

We have demonstrated that self-assembled peptide nanostructures can be developed as a ratiometric fluorescence biosensor to measure and quantify ligand-induced conformational transition behaviors. This SPN biosensor combines the concept of dynamic self-assembly, helix-coil transition, and allostery. Biomacromolecular interactions such as protein-RNA, protein-DNA, and protein-protein interactions are involved in numerous cellular communications and a number of disease pathways. Because they occur between large biological macromolecules, comparatively large biosensors should be more suitable for binding to typically wide and/or shallow interfaces of biomacromolecular interactions. Therefore, this SPN biosensor should be useful in detecting α-helix-mediated biomacromolecular interactions.

ASSOCIATED CONTENT

Supporting Information.

Chemical structures, mass spectra, HPLC chromatograms, additional data, and experimental procedures. This material is available free of charge via the Internet at http://pubs.acs.org.

AUTHOR INFORMATION

Corresponding Author

*E-mail: yblim@yonsei.ac.kr; Tel.: +82-2-2123-5836; Fax: +82-2-312-5375.

Notes

The authors declare no competing financial interest.

ACKNOWLEDGMENT

This work was supported by grants from the National Research Foundation (NRF) of Korea (2012R1A1A2006453, 2009-0083522, 2013M2B2A4041202, 2009-0066736).

REFERENCES

(1) Oh, K. J.; Cash, K. J.; Plaxco, K. W. *J. Am. Chem. Soc.* **2006**, *128*, 14018-14019.

(2) Esser, B.; Schnorr, J. M.; Swager, T. M. *Angew. Chem. Int. Ed.* **2012**, *51*, 5752-5756.

(3) Gonzalez, D. C.; Savariar, E. N.; Thayumanavan, S. *J. Am. Chem. Soc.* **2009**, *131*, 7708-7716.

(4) Thurley, S.; Roglin, L.; Seitz, O. *J. Am. Chem. Soc.* **2007**, *129*, 12693-12695.

(5) Yang, Y.; Seidlits, S. K.; Adams, M. M.; Lynch, V. M.; Schmidt, C. E.; Anslyn, E. V.; Shear, J. B. *J. Am. Chem. Soc.* **2010**, *132*, 13114-13116.

(6) Miranda, O. R.; Li, X.; Garcia-Gonzalez, L.; Zhu, Z. J.; Yan, B.; Bunz, U. H.; Rotello, V. M. *J. Am. Chem. Soc.* **2011**, *133*, 9650-9653.

(7) Zhuang, Y. D.; Chiang, P. Y.; Wang, C. W.; Tan, K. T. *Angew. Chem. Int. Ed.* **2013**, *52*, 8124-8128.

(8) Nakano, S.; Fukuda, M.; Tamura, T.; Sakaguchi, R.; Nakata, E.; Morii, T. *J. Am. Chem. Soc.* **2013**, *135*, 3465-3473.

(9) Huang, Y. J.; Ouyang, W. J.; Wu, X.; Li, Z.; Fossey, J. S.; James, T. D.; Jiang, Y. B. *J. Am. Chem. Soc.* **2013**, *135*, 1700-1703.

(10) Ma, D. L.; Chan, D. S.; Man, B. Y.; Leung, C. H. *Chem-Asian J.* **2011**, *6*, 986-1003.

(11) He, H. Z.; Leung, K. H.; Wang, W.; Chan, D. S.; Leung, C. H.; Ma, D. L. *Chem. Commun.* **2014**, *50*, 5313-5315.

(12) Giver, L.; Gershenson, A.; Freskgard, P. O.; Arnold, F. H. *Proc. Natl. Acad. Sci. U.S.A.* **1998**, *95*, 12809-12813.

(13) Munoz, V. *Annu. Rev. Biophys. Biomol. Struct.* **2007**, *36*, 395-412.

(14) Pless, S. A.; Ahern, C. A. *Annu. Rev. Pharmacol. Toxicol.* **2013**, *53*, 211-229.

(15) Dyson, H. J.; Wright, P. E. *Chem. Rev.* **2004**, *104*, 3607-3622.

(16) Han, S.; Kim, D.; Han, S. H.; Kim, N. H.; Kim, S. H.; Lim, Y. B. *J. Am. Chem. Soc.* **2012**, *134*, 16047-16053.

(17) Fletcher, J. M.; Harniman, R. L.; Barnes, F. R.; Boyle, A. L.; Collins, A.; Mantell, J.; Sharp, T. H.; Antognozzi, M.; Booth, P. J.; Linden, N.; Miles, M. J.; Sessions, R. B.; Verkade, P.; Woolfson, D. N. *Science* **2013**, *340*, 595-599.

(18) Apostolovic, B.; Danial, M.; Klok, H. -A. *Chem. Soc. Rev.* **2010**, *39*, 3541-3575.

(19) Lowik, D. W.; Leunissen, E. H.; van den Heuvel, M.; Hansen, M. B.; van Hest, J. C. *Chem. Soc. Rev.* **2010**, *39*, 3394-3412.

(20) Reches, M.; Gazit, E. *Science* **2003**, *300*, 625-627.

(21) Jeong, W. J.; Choi, S. J.; Choi, J. S.; Lim, Y. B. *ACS Nano* **2013**, *7*, 6850-6857.

(22) Micklitsch, C. M.; Knerr, P. J.; Branco, M. C.; Nagarkar, R.; Pochan, D. J.; Schneider, J. P. *Angew. Chem. Int. Ed.* **2011**, *50*, 1577-1579.

(23) Capito, R. M.; Azevedo, H. S.; Velichko, Y. S.; Mata, A.; Stupp, S. I. *Science* **2008**, *319*, 1812-1816.

(24) Gradisar, H.; Bozic, S.; Doles, T.; Vengust, D.; Hafner-Bratkovic, I.; Mertelj, A.; Webb, B.; Sali, A.; Klavzar, S.; Jerala, R. *Nat. Chem. Biol.* **2013**, *9*, 362-366.

(25) Lim, Y. B.; Moon, K. S.; Lee, M. *Chem. Soc. Rev.* **2009**, *38*, 925-934.

(26) Pollard, V. W.; Malim, M. H. *Annu. Rev. Microbiol.* **1998**, *52*, 491-532.

(27) Jain, C.; Belasco, J. G. *Cell* **1996**, *87*, 115-125.

(28) Jain, C.; Belasco, J. G. *Mol. Cell.* **2001**, *7*, 603-614.

(29) Casu, F.; Duggan, B. M.; Hennig, M. *Biophys. J.* **2013**, *105*, 1004-1017.

(30) Daugherty, M. D.; Liu, B.; Frankel, A. D. *Nat. Struct. Mol. Biol.* **2010**, *17*, 1337-1342.

(31) Daly, T. J.; Rusche, J. R.; Maione, T. E.; Frankel, A. D. *Biochemistry* **1990**, *29*, 9791-9795.

(32) Battiste, J. L.; Mao, H.; Rao, N. S.; Tan, R.; Muhandiram, D. R.; Kay, L. E.; Frankel, A. D.; Williamson, J. R. *Science* **1996**, *273*, 1547-1551.

(33) DiMattia, M. A.; Watts, N. R.; Stahl, S. J.; Rader, C.; Wingfield, P. T.; Stuart, D. I.; Steven, A. C.; Grimes, J. M. *Proc. Natl. Acad. Sci. U.S.A.* **2010**, *107*, 5810-5814.

(34) Fang, X.; Wang, J.; O'Carroll, I. P.; Mitchell, M.; Zuo, X.; Wang, Y.; Yu, P.; Liu, Y.; Rausch, J. W.; Dyba, M. A.; Kjems, J.; Schwieters, C. D.; Seifert, S.; Winans, R. E.; Watts, N. R.; Stahl, S. J.; Wingfield, P. T.; Byrd, R. A.; Le Grice, S. F.; Rein, A.; Wang, Y. X. *Cell* **2013**, *155*, 594-605.

(35) Han, S. H.; Lee, M. K.; Lim, Y. B. *Biomacromolecules* **2013**, *14*, 1594-1599.

(36) Wang, D.; Chen, K.; Kulp Iii, J. L.; Arora, P. S. *J. Am. Chem. Soc.* **2006**, *128*, 9248-9256.

(37) Daugherty, M. D.; Booth, D. S.; Jayaraman, B.; Cheng, Y.; Frankel, A. D. *Proc. Natl. Acad. Sci. U.S.A.* **2010**, *107*, 12481-12486.

(38) Lim, Y. B.; Lee, E.; Lee, M. *Angew. Chem. Int. Ed.* **2007**, *46*, 3475-3478.

(39) Bains, G. K.; Kim, S. H.; Sorin, E. J.; Narayanaswami, V. *Biochemistry* **2012**, *51*, 6207-6219.

(40) Turro, N. J.; Kuo, P.-L. *Langmuir* **1986**, *2*, 438-442.

(41) Tan, R.; Chen, L.; Buettner, J. A.; Hudson, D.; Frankel, A. D. *Cell* **1993**, *73*, 1031-1040.

Table of Contents (TOC) graphic

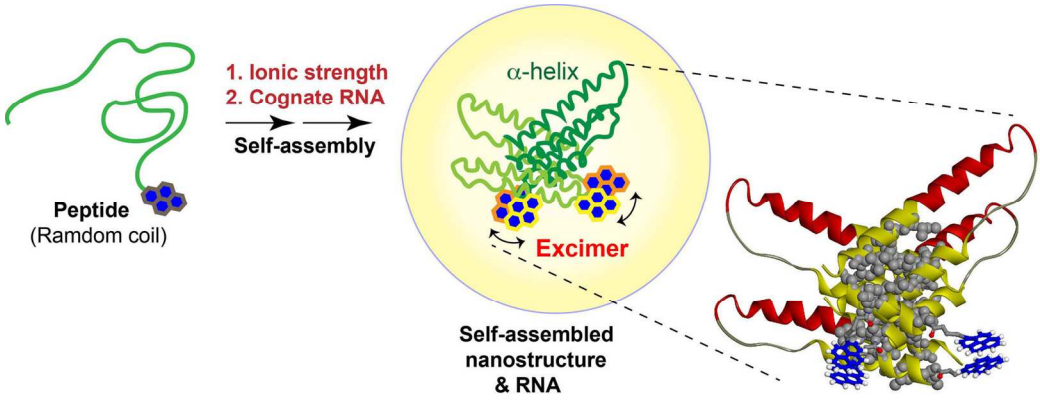

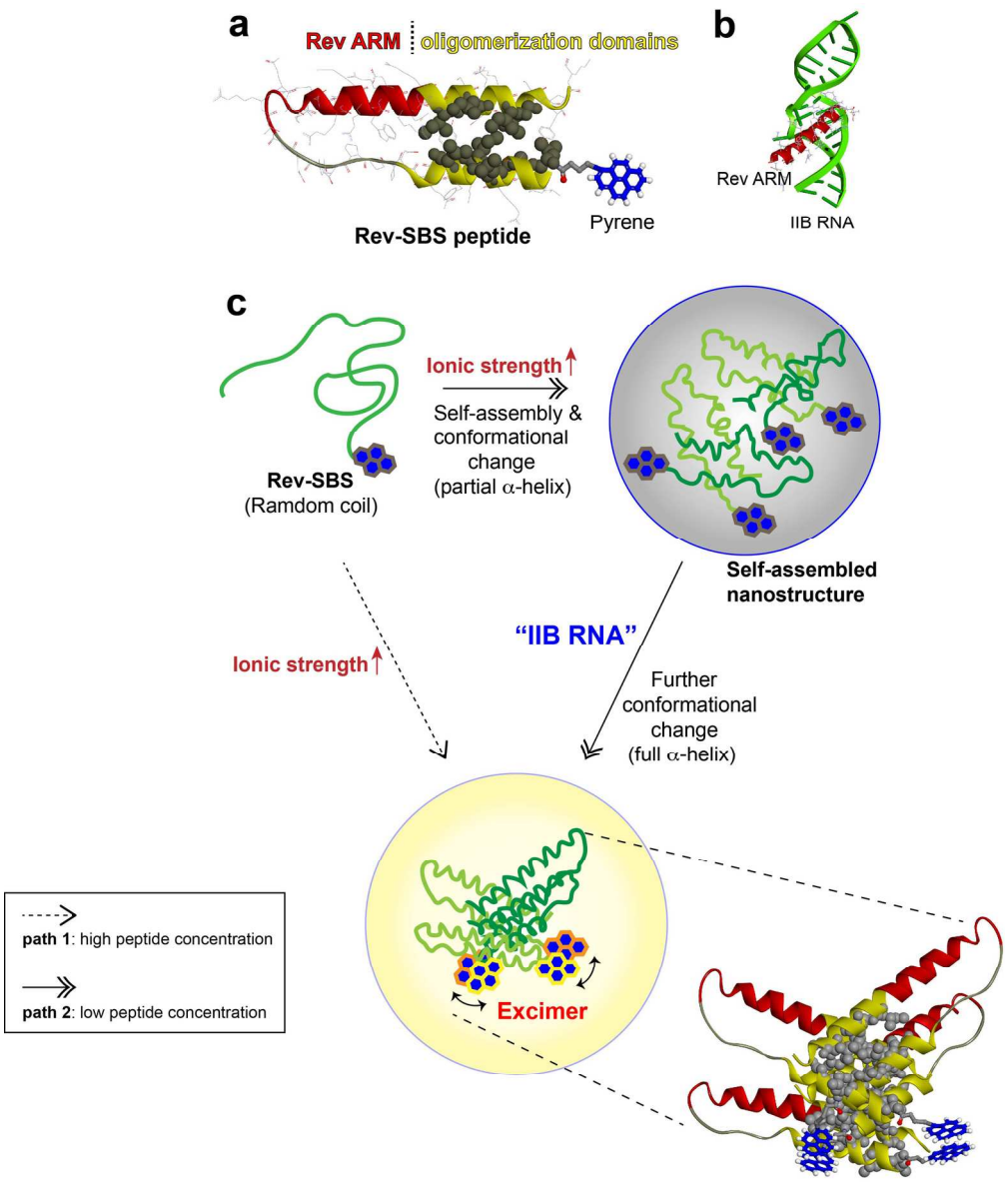

176x208mm (300 x 300 DPI)

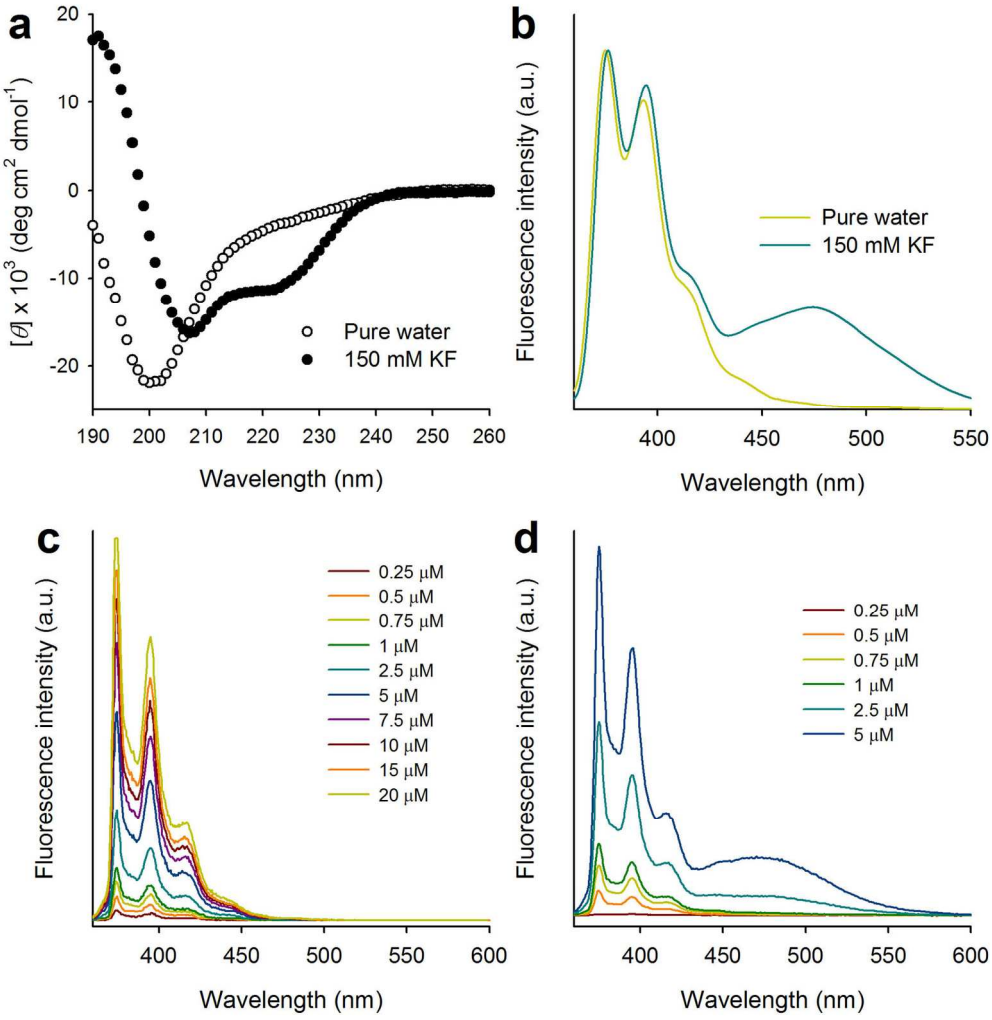

84x87mm (600 x 600 DPI)

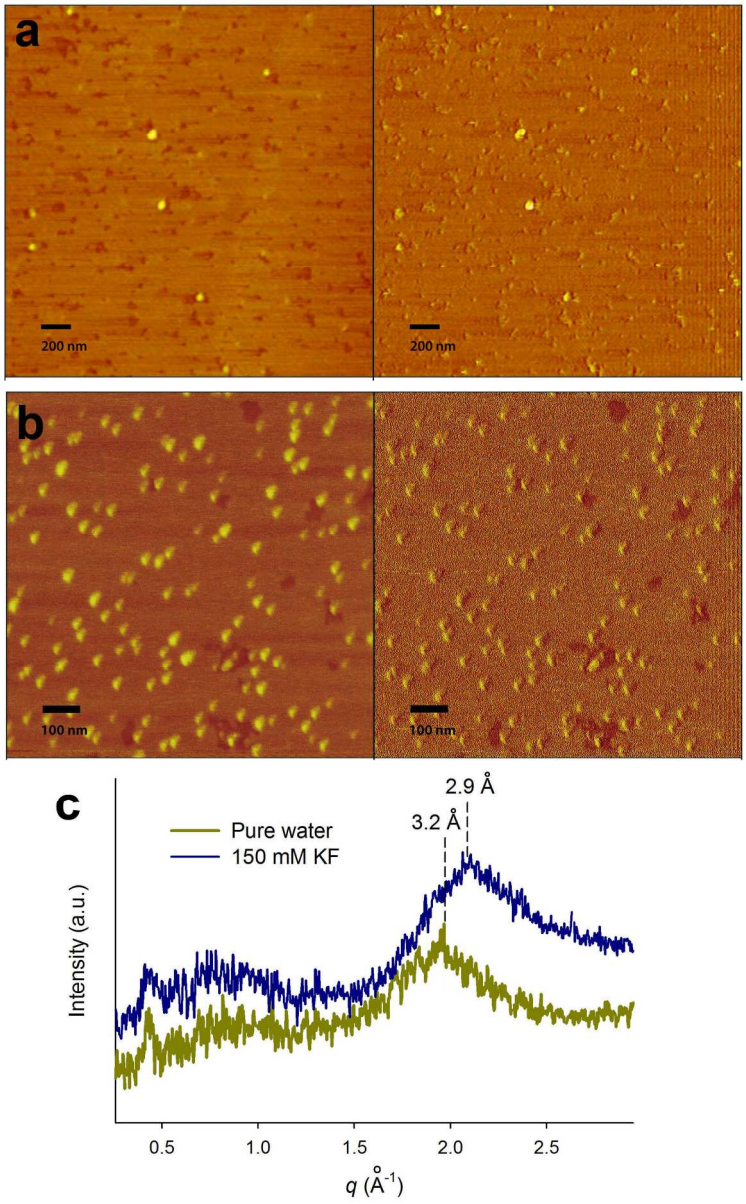

131x208mm (600 x 600 DPI)

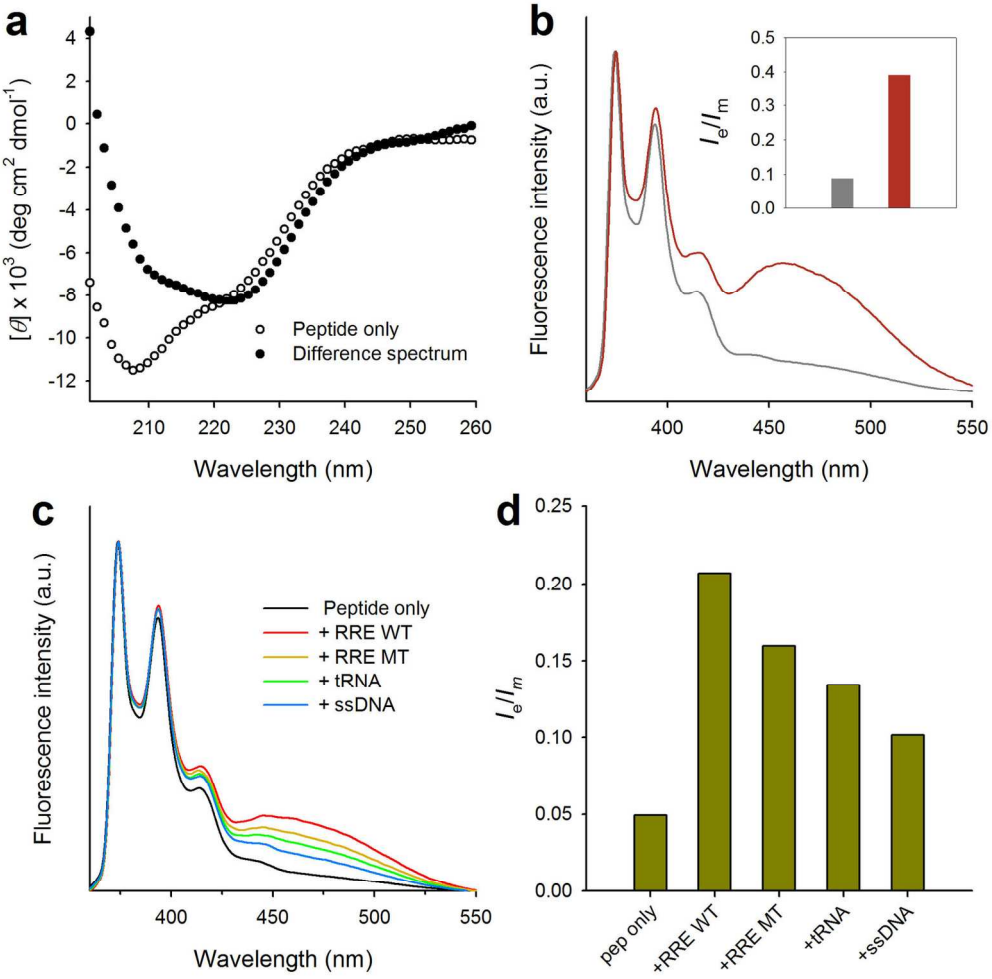

81x79mm (600 x 600 DPI)

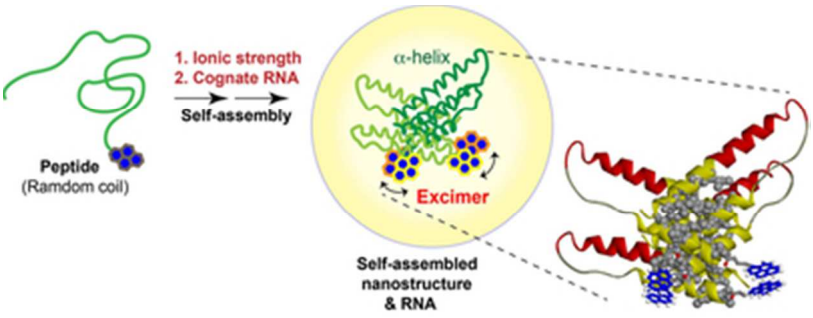

34x13mm (300 x 300 DPI)